Does the unification
of BL Lac and FR I radio galaxies require jet velocity structures?

M. Chiaberge[1]**, A. Celotti**[1]**, A. Capetti**[2]**, and G. Ghisellini**[3]

[1] SISSA/ISAS, Via Beirut 2-4, 34014 Trieste, Italy
[2] Osservatorio Astronomico di Torino, Strada Osservatorio 20, 10025 Pino Torinese, Italy
[3] Osservatorio Astronomico di Brera, Via Bianchi 46, 23807 Merate (LC), Italy

Abstract. We explore the viability of the unification of BL Lacs and FR I radio galaxies by comparing the core emission of radio galaxies with those of BL Lacs of similar extended radio power, taking advantage of the newly measured optical nuclear luminosity of FR I sources. The spectral properties of complete samples are also studied in the radio-optical luminosity plane: starting from the Spectral Energy Distribution (SED) of BL Lacs, we calculate the predicted luminosity of FR I nuclei in the frame of a simple one–zone model, by properly taking into account the relativistic transformations. We find that the bulk Lorentz factors required by the spread in the observed luminosities in all bands are significantly smaller than those implied by other, both observational and theoretical, considerations. This discrepancy is also reflected in the fact that FR I nuclei are over–luminous by a factor of 10–10^4, with respect to the predictions, both in the radio and in the optical band.

In order to reconcile these results with the unification scheme, velocity structures in the jet are suggested, where a fast spine is surrounded by a slow (but still relativistic) layer so that the emission at different angles is dominated by different velocity components: the fast one dominates the emission in BL Lacs while the slow layer dominates the emission in misaligned objects. Furthermore for the lowest luminosity BL Lacs it has to be also postulated that their beaming factor in the radio band is lower than in the optical (and X–ray), as would result from deceleration of the jet.

The self–consistency of the unification model therefore requires that both intrinsic differences in the SED and different beaming properties play a substantial role in characterizing the phenomenology of these sources.

Key words: galaxies: active – galaxies: BL Lacertae objects: general – galaxies: jets – galaxies: nuclei

1. Introduction

Unification models adduce the main differences between the observed properties of different classes of AGNs to the anisotropy of the radiation emitted by the active nucleus (see Antonucci 1993 and Urry & Padovani 1995 for reviews). In particular, for low luminosity radio-loud objects, namely BL Lacs and FR I radio galaxies (Fanaroff & Riley 1974), it is believed that this effect is mainly due to relativistic beaming. In fact, there is growing evidence that obscuration does not play a significant role in these objects, contrary to other classes of AGNs. This is indicated by optical (Chiaberge et al. 1999 hereafter Paper I), radio (Henkel et al. 1998), and X-ray information (e.g. Fabbiano et al. 1984, Worral & Birkinshaw 1994, Trussoni et al. 1999). Within this scenario, the emission from the inner regions of a relativistic jet dominates the observed radiation in BL Lacs, while in FR I, whose jet is observed at larger angles with respect to the line of sight, this component is strongly debeamed. Evidence for this unification scheme includes the power and morphology of the extended radio emission of BL Lacs (e.g. Antonucci & Ulvestad 1985, Kollgaard et al. 1992, Murphy et al. 1993) and the properties of their host galaxies (e.g. Ulrich 1989, Stickel et al. 1991, Urry et al. 1999), which are similar to those of FR I. Furthermore, there is a quantitative agreement among the amount of beaming required by different observational properties (e.g. Ghisellini et al. 1993), the number densities and luminosity functions of the parent and beamed populations in different bands (e.g. Urry & Padovani 1995, Celotti et al. 1993) and the comparison of the radio core emission of beamed and unbeamed objects with similar total radio power (Kollgaard et al. 1996).

Despite this global agreement, it should be stressed that beaming factors inferred from the broad band spectral properties of blazars, more specifically superluminal motions, transparency to the γ–ray emission, shape of the SED and time–lags among variations at different frequencies, are significantly and systematically larger than those suggested by radio luminosity data (Dondi & Ghisellini 1995, Ghisellini et al. 1998, Tavecchio et al. 1998).

Thanks to the Hubble Space Telescope (HST), faint optical nuclear components have been recently detected in FR I galaxies (Chiaberge et al. 1999). A strong linear correlation is found between this optical and the radio core emission which strongly argues for a common non-thermal origin. This suggests that the optical cores can be identified with synchrotron radiation pro-

duced in a relativistic jet, qualitatively supporting the unifying model for FR I and BL Lacs.

These information offer a new possibility of verifying the unification scheme, by directly comparing the properties of the optical and radio cores of radio galaxies with their putative aligned (beamed) counterparts, analogously to the procedure followed for the radio cores. X-ray observations also provide useful constraints to the nuclear emission of FR I sources (e.g. Hardcastle & Worrall 1999).

The main advantage of using multifrequency data is the possibility of directly comparing the full broad band spectral distributions of these two classes of sources and eventually shed light on the apparent discrepancy in the Lorentz factors inferred from different approaches.

The paper is organized as follows. The (complete) samples of BL Lacs and radio galaxies are presented in Sect. 2. In Sect. 3 we compare separately the core radio and optical emission of beamed and unbeamed objects with similar extended radio power. From this we infer the Lorentz factors requested by the unification scheme within the simplest scenario in which the radiation is emitted by a single uniform region of the relativistic jet. In Sect. 4 the radio and optical data are considered together and, starting from the observed SED of BL Lacs, we derive the expected properties of the nuclear emission of FR I, by taking into account the spectral dependence of the relativistic transformations. As the single–region picture does not account for the observed properties, in Sect. 5 we explore a (simple) alternative scenario and test it also against the X-ray information. Summary and conclusions are presented in Sect. 6.

2. The samples

2.1. FR I radio galaxies

Our complete sample of radio galaxies comprises all the FR I sources belonging to the 3CR catalogue (Spinrad et al. 1985), morphologically identified as FR I. The redshifts of these objects span the range $z = 0.0037 - 0.29$, with a median value of $z = 0.03$, and the total radio luminosities at 1.4 GHz are between $10^{30.2}$ and $10^{34.2}$ erg s^{-1} Hz^{-1} ($H_0 = 75$ km s^{-1} Mpc^{-1} and $q_0 = 0.5$ are adopted hereafter). We exclude from the original sample the peculiar object 3C 386, as discussed in Paper I. The optical and radio data are from Paper I, while the X-ray ones from Hardcastle & Worral (1999). The optical data are extrapolated to the V band using a spectral index $\alpha_o = 1$ ($F_\nu \propto \nu^{-\alpha}$).

2.2. Radio and X-ray selected BL Lacs samples

We consider both the complete sample of 34 radio selected BL Lacs derived from the 1Jy catalog (Stickel et al. 1991, Kühr et al. 1981), and the BL Lac sample selected from the *Einstein* Slew survey (Elvis et al. 1992, Perlman et al. 1996), which comprises 48 objects, and it is nearly complete. The extended radio power (at 1.4 GHz) $L_{\rm ext}$ [erg s^{-1} Hz^{-1}] spans the ranges $10^{30.1}-10^{33.8}$ (1Jy BL Lacs, Kollgaard et al. 1996) and $10^{29.1}-10^{33.4}$ (Slew survey BL Lacs, Kollgaard et al. 1996, Perlman

et al. 1996); the redshifts are between 0.049 and 1.048 (median $z = 0.501$) and between 0.031 and 0.513 (median $z = 0.188$) for the two samples, respectively (the redshifts of the Slew BL Lacs are taken from the data collected by Fossati et al. 1998).

Instead of classifying BL Lacs according to their selection spectral band, in the following we adopt the definitions of high and low energy peaked BL Lacs (HBL and LBL respectively), which are based on the position of the (synchrotron) emission peak in the spectrum and therefore more indicative of the physical characteristics of the objects (Giommi & Padovani 1994, Fossati et al. 1998). Of the 34 objects belonging to the 1 Jy sample, 32 are classified as LBL and 2 as HBL, while of the 48 X-ray selected BL Lacs, 40 are HBL and 8 are LBL.

The spectral data for both samples of BL Lacs are taken from Fossati et al. 1998.
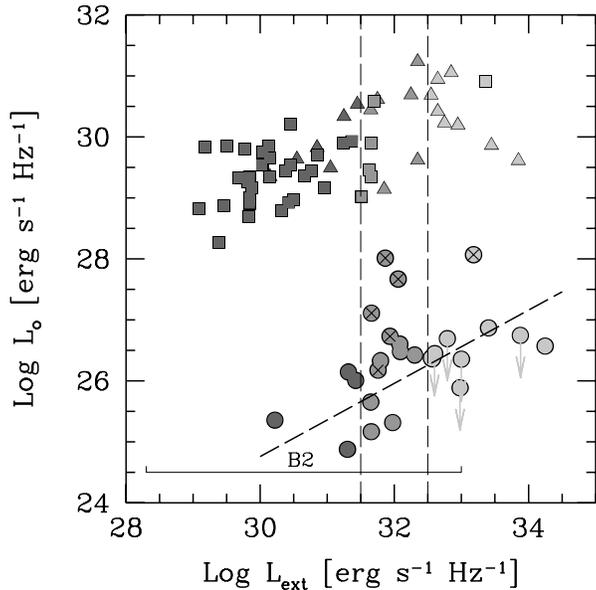
3. Core versus extended luminosity

According to the unification models the beamed and unbeamed populations must cover the same range of extended luminosity, as this is considered to be isotropic. On the contrary, emission from the core is affected by beaming: radio galaxies should have a fainter central component, whose intensity would depend on the Doppler factor $\delta = [\Gamma(1 - \beta \cos\theta)]^{-1}$, where $\Gamma = (1 - \beta^2)^{-1/2}$, βc is the bulk velocity of the emitting plasma and θ the angle between the direction of the jet and the line of sight. The transformation law for the specific flux density is in fact $F_\nu = \delta^{p+\alpha} F'_\nu$, where the primed quantity refers to the comoving frame, α is the local spectral index, $p = 2$ for a continuous jet and $p = 3$ for a moving sphere.

Therefore the comparison of the core emission of beamed objects and their parent population with similar extended emission provides a direct estimate of the Lorentz factor of the radiating plasma, if the typical observing angles are known. With this aim and similarly to what has been done in the radio band (e.g. Kollgaard et al. 1996), we plot the optical V band luminosity (L_o) vs the extended radio luminosity at 1.4 GHz ($L_{\rm ext}$) for the three samples (Fig. 1).

First we should note that the HBL objects do not fully share the range of extended radio power of the 3CR radio galaxies (the HBL total luminosities are in fact more similar to the objects belonging to the B2 sample of low power radio galaxies). Conversely, $L_{\rm ext}$ of LBL well match those FR I of the 3CR catalog.

Also notice that the regions occupied by the two samples of BL Lacs appear to be continuously connected, the lower radio power BL Lacs (which are HBLs) and the higher radio power ones (LBLs) having an optical luminosity which weakly increases for increasing extended luminosity. Because of this trend, in order to compare sources with the same $L_{\rm ext}$ we have sub-divided the samples into three bins, namely: $\log L_{\rm ext}$ [erg s^{-1} Hz^{-1}] < 31.5, $\log L_{\rm ext}$ between 31.5 and 32.5, and $\log L_{\rm ext} > 32.5$.

We thus calculate the median values of the observed nuclear luminosity of FR I and BL Lacs in each interval of extended power. BL Lacs are on average 4 orders of magnitude brighter

Fig. 1. Optical core luminosity (V band) versus radio extended luminosity at 1.4 GHz for FR I (circles), HBLs (squares) and LBLs (triangles). The grey scale refers to the three bins of extended radio power. The dashed line represents the linear fit to the FR I sample, having excluded the most aligned sources, here marked with crosses (see text). The range of extended power covered by the B2 sample of radio galaxies is also indicated.
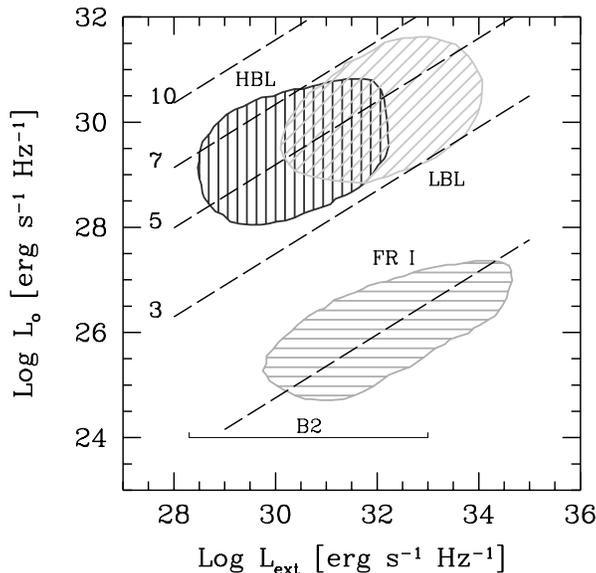
Fig. 2. The regions occupied by the three samples in the optical luminosity versus extended radio luminosity plane, as for Fig. 1. The dashed lines indicate the correlation found between these two quantities when shifted by beaming effects for the values of the bulk Lorentz factor marked on the left.

than FR I cores. We can assume that BL Lacs are observed[1] at $\theta \sim 1/\Gamma$ and FR Is at $\theta = 60°$: in fact, for an isotropic distribution of objects, $\theta = 60°$ corresponds to the median angle

---

[1] At the particular angle $\theta \sim 1/\Gamma$, one obtains $\delta = \Gamma$.
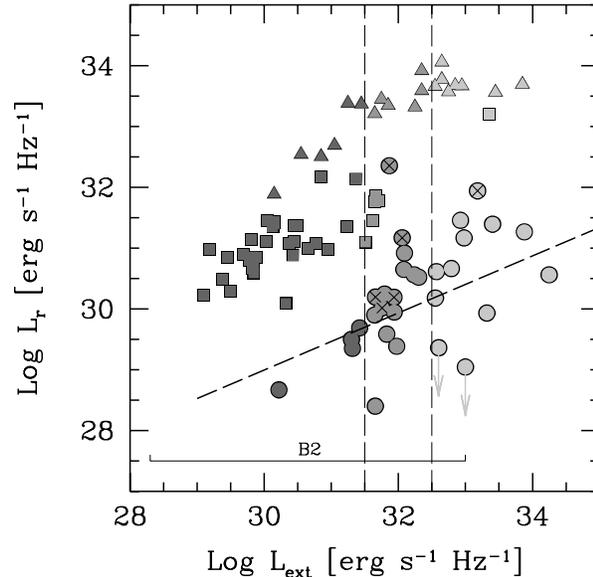
Fig. 3. Radio core luminosity (at 5 GHz) versus radio extended luminosity at 1.4 GHz for FR I (circles), X-ray selected (squares) and radio-selected BL Lacs (triangles). The dashed line is the correlation between these two quantities found for a larger sample of galaxies by Giovannini et al. (1988) and converted to 1.4 GHz using $\alpha_r = 0.7$.

if, as it is in the case of FR I, the scatter in the optical luminosity is dominated by relativistic beaming. Bulk Lorentz factors $\Gamma \sim 4$ for the case of an emitting sphere and ~ 6 for a continuous jet are required in order to account for the different core luminosities of FR I and BL Lacs in each bin of extended power. An optical spectral index $\alpha_o = 1$ is assumed for all sources (independent of beaming).

An alternative method to estimate Γ relies on the fact that, for a randomly oriented sample, the best fit regression line of a luminosity distribution corresponds to the behavior of sources observed at $\sim 60°$, once the most core dominated objects are excluded (Kollgaard et al. 1996). We thus determine the best fit regression of FR I in the $L_{ext} - L_o$ plane, after excluding from the sample the 5 objects in which optical jets are detected. These sources, in fact, have the most luminous optical cores, are among the most core dominated objects in the radio band, and their radio jets are shorter, indicating that they are pointing towards the observer (Sparks et al. 1995). Interestingly, we obtain that there is a remarkable correlation ($P > 99.9\%$) between $\log L_{ext}$ and $\log L_o$, among the remaining 20 "highly misoriented" objects, although with a slope (~ 0.6) marginally steeper than the correlation between L_{ext} and core radio luminosity (L_r) found by Giovannini et al. (1988) for a larger sample of radio galaxies. In Fig. 2 we show the regions in which the three samples are located in the $L_{ext} - L_o$ plane, and the dashed lines represent the "beamed" FR I population as observed under an angle $\sim 1/\Gamma$ in the case of $p = 3$. Also with this method $\Gamma \sim 5$ (~ 7) are required to displace the FR I to the regions occupied by both HBL and LBL for $p = 3$ ($p = 2$).

Let us now consider L_r (at 5 GHz) versus L_{ext} (Fig. 3), analogously to what is shown by Kollgaard et al. (1996) for a larger

sample of radio galaxies (which also includes our objects). The typical radio core luminosities of HBL and LBL are significantly different, the latter objects being on average about one order of magnitude more luminous than the former ones. Conversely, as we have already pointed out, no substantial difference between the two classes is found in the case of L_o.

These results have been initially attributed to a different amount of beaming for X-ray and radio-selected BL Lacs (i.e. different angle of sight and/or different jet velocities[2]) while more recently a consistent picture has emerged where this diversity can be accounted for by the different shape of their intrinsic SED (e.g. Padovani 1992, Ghisellini & Maraschi 1989, Giommi & Padovani 1994, Fossati et al. 1998). The role of these two scenarios will be further explored in the next section, through the comparison of the SED of both types of BL Lacs with their parents.

We conclude that the Lorentz factors inferred from the comparison of the radio, but also optical emission of FR I and BL Lacs, are consistent with those previously estimated from the statistics of these sources within the unifying scheme. However, as already mentioned, such values are significantly and systematically lower than those required by other independent means, such as superluminal motions and high energy spectral constraints (fit to the overall SED and time–lags) in both LBLs and HBLs. (Maraschi et al. 1992, Sikora et al. 1994, Celotti et al. 1998, Tavecchio et al. 1998). These latter methods require a value of the Doppler factor δ in the range 15–20 for the region emitting most of the radiation in both HBLs and LBLs. The need for high degrees of beaming will constitute a crucial point in the following.

4. FR I and BL Lac in the L_o and L_r plane

Since for the first time multifrequency data are available also for the nucleus of radio galaxies, we can now directly compare the spectral properties of beamed objects and their parent population: this new approach can thus combine information from the SED of BL Lacs with those inferred from their relation with FR I. In particular in Paper I and in Chiaberge et al. 2000 we showed how the location of sources in the L_o and L_r plane represents a very useful tool to discuss their nuclear properties. In Fig. 4 we show the optical vs radio core luminosity for the three samples. The dashed line represents the (almost linear) correlation found between these two quantities among the FR I sources (Paper I). Radio galaxies, HBL and LBL occupy different regions of this plane: LBLs are located only marginally above the continuation of this correlation, while HBL are ~ 2 order of magnitude brighter in the optical with respect to other objects for a given radio luminosity.

In order to determine how beaming affects the observed luminosities and thus how objects could be connected in this plane, we consider the SED of BL Lacs, observationally much better determined, and calculate the observed spectrum of the
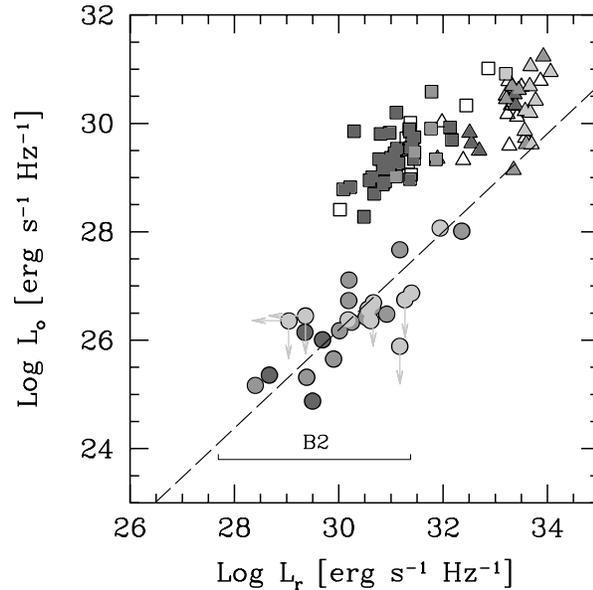
Fig. 4. BL Lacs and FR I radio galaxies in the $L_r - L_o$ plane. Empty symbols are objects with no data on their extended radio power, filled symbols and grey scale are as in Fig. 1. The dashed line is the radio-optical core correlation (Paper I). The range of core luminosity of the B2 radio galaxies is also reported. Notice that the B2 cores could at most extend this correlation by ~ 1 order of magnitude towards lower luminosities.

misaligned objects, by taking into account relativistic transformations.

In fact, an important point, previously neglected, is that these transformations depend on the spectral index in the band considered, which in itself might change as a function of the degree of beaming. Therefore, in order to correctly de–beam the SED of BL Lacs, a continuous representation of it and an estimate of the bulk Lorentz factor of the emitting region are needed (it is again assumed $\theta = 1/\Gamma$). While any continuous description of the SED and typical Lorentz factors can be used, we derive both of them by adopting a homogeneous synchrotron self–Compton emission model to reproduce the observed SEDs (e.g. Chiaberge & Ghisellini 1999, Ghisellini et al. 1998, Mastichiadis & Kirk 1997). This approach has the advantage of considering both the emission and dynamical (Γ) properties self–consistently.[3] The bulk velocities obtained in this way are fully compatible with those inferred from the already mentioned constraints (Sect. 3).

Let us firstly consider single objects for which the SED is well sampled, namely Mkn 421 (a typical HBL) and PKS 0735+178 (a typical LBL). We model the observed SED as explained, derive the value of $\Gamma(=\delta)$ for the two sources and then calculate their corresponding observed SEDs for different orientations. Clearly the net effect of debeaming is a "shift" of the SED towards lower luminosities and energies (see Fig. 5).

---

[2] If so the inferred Lorentz factors, relative to our sample, are $\Gamma = 4$ (3) for HBL $\Gamma = 10$ (5) for LBL, in the case of p=2 (p=3)

[3] These models, in fact, satisfy time variability constraints, assume continuous injection of particles, radiative and adiabatic cooling, γ–γ collisions and pair production. The continuous curves shown in Fig. 5 are then not only interpolating curves, but physically possible fits to the data.
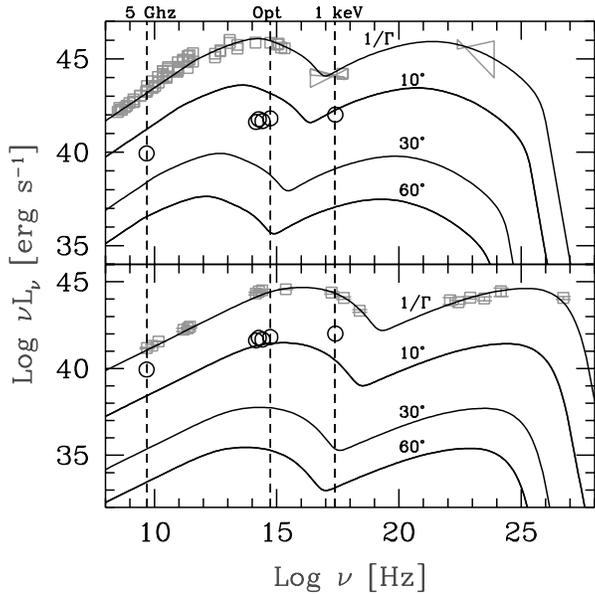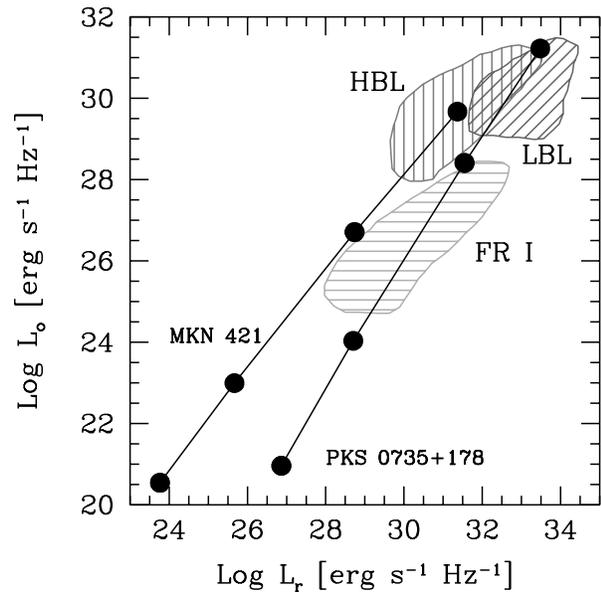
Fig. 5. Spectral energy distributions of Mkn 421 (lower panel) and PKS 0735+178 (top panel) and debeamed SED for different viewing angles in the case of a single emitting component. The Lorentz factors inferred for the two sources are $\Gamma = 20$ and $\Gamma = 16$, respectively. For comparison, we report (empty circles) the radio, IR and optical (HST) and X-ray (ROSAT) data for 3C 264 (Capetti et al. 2000). The (non-simultaneous) data for PKS 0735+178 are taken from the literature (NED). The (quasi-simultaneous) data for Mkn 421 are from Macomb et al. (1996).
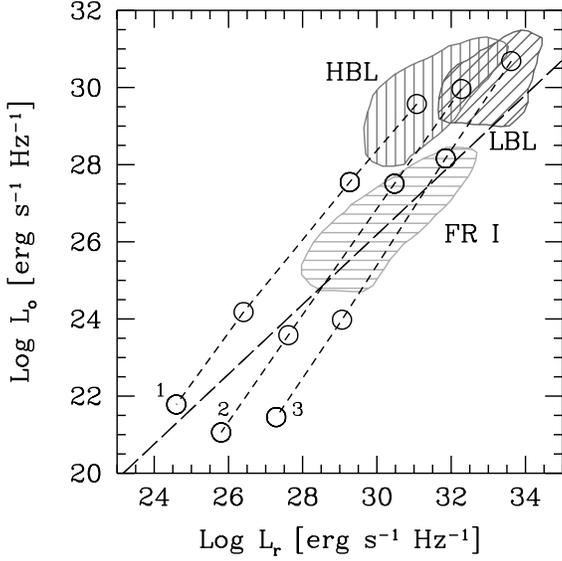

Fig. 6. Debeaming trails in the radio-optical luminosity plane for Mkn 421 and PKS 0735+178, in the frame of a single emitting region model. The filled circles correspond to the predicted luminosities of objects at different viewing angles. Top to bottom: $\theta = 1/\Gamma$, $10°$, $30°$ and $60°$.

Notice that, as the model is appropriate for the optically thin part of the spectrum, in order to account for the radio emission, which necessarily has to be produced on larger scales, we linearly extrapolate the fit from the infrared-mm spectral region. However, at an angle of $\theta = 60°$ and for the Lorentz factors derived from the model, $\Gamma \sim 15$–20, the observed (debeamed) radiation at 5 GHz corresponds to what is seen in BL Lacs at far infrared frequencies (respectively ~ 500–$300\,\mu$m, see Fig. 5) and therefore the debeamed points in Fig. 6 represent the correct predicted luminosities of the BL Lac component at 5 GHz.

The resulting debeamed optical and radio luminosities are reproduced in Fig. 6. The lines represent "debeaming trails" and the filled circles the calculated debeamed luminosities for $\theta = 1/\Gamma$ (i.e. the BL Lac itself), $10°$, $30°$ and $60°$. Most noticeably, for $\theta = 60°$ – which is the mean angle of sight for the misaligned population – the BL Lac component is about four orders of magnitude below the radio galaxy region in the optical, and one/four in the radio band.

While equivalently incompatible with the FR I population, the HBL and LBL move on different trails. This is due to the different shape of their SED (see Fig. 5), and in particular to the position of the synchrotron peak frequency: if – for increasing values of θ – in the rest frame the peak overcomes the optical band, the spectral index steepens and the optical flux drops more rapidly than the radio one.

Another remarkable result is that the debeaming trail of the HBL does not even cross the region occupied by radio galaxies

in the $L_r - L_o$ plane. As this might be a serious problem for the unified scheme, we further examine this issue. In particular we closely examine the effect of the spectral shape and its relation with the intrinsic luminosity by considering three different SED, which represent the whole family of BL Lacs, from HBLs to LBLs.[4] In Fig. 7 we plot the resulting trails: once again, as in the cases of Mkn 421 and PKS 0735+178, the expected nuclear luminosity is 10–10^4 times fainter than what observed in FR I and the debeaming trail for the lower luminosity object (a typical HBL) does not even cross the FR I region. Note that if the luminosity is indeed related to the shape of the SED, this discrepancy would exacerbate for even fainter BL Lacs. In fact for HBL the radio and optical spectral slopes can be considered constant as the viewing angle increases, resulting in a linear (one to one) debeaming trail, parallel to the FR I correlation.

Summarizing: the radio and optical luminosities of BL Lacs and FR I are not consistent with the simplest predictions of the unifying scheme, if a single emitting region is responsible for the different broad band spectral properties of the beamed and parent populations. More specifically: i) Lorentz factors ~ 15, as derived from the high energy spectral properties, underestimate the predicted emission from the parent population; ii) the relative ratio of radio to optical luminosity of HBL is inconsistent with the observed FR I spectra. In the next section we discuss and test a possible solution to these discrepancies.

---

[4] The three SED correspond to different bins of radio luminosity (at 5 GHz) – which appears correlated with the bolometric luminosity and the position of the peak frequency (Fossati et al. 1998, Ghisellini et al. 1998).

Fig. 7. Debeaming trails in the radio-optical luminosity plane for average BL Lacs SED, in the frame of a single emitting component model. The filled circles correspond to the predicted optical-radio luminosity for different angles of sight (top to bottom: $\theta = 1/\Gamma$, $10°$, $30°$ and $60°$).

5. A jet velocity structure

We have shown that the high bulk Lorentz factors required by the emission models of BL Lacs imply that if such objects are observed at $60°$ the resulting spectral properties are not compatible with what is observed in the nuclei of radio galaxies. And indeed the previous comparison of the core emission of FR I and BL Lacs (see Sect. 3) led to lower values of Γ. How can these results be reconciled within the unifying scenario? A possible and plausible effect, which could account for this discrepancy, is provided by the existence of a distribution in the bulk velocity of the flow, with the emission from plasma moving at different speeds dominating the flux observed at different viewing angles.

Let us consider this hypothesis in the frame of the unification scheme and examine the simplest case, i.e. a model with two axisymmetric components having the same intrinsic luminosity and spectra. In other words, the only difference between the center and the layer of the jet is the bulk Lorentz factor which is determined for the *spine* (Γ_{spine}) by modeling the BL Lac SED, while for the *layer* (Γ_{layer}) by requiring that the debeamed BL Lac match the FR I distributions in the $L_{\text{ext}} - L_o$ and $L_r - L_o$ planes.

The monochromatic intensity emitted by the jet is therefore calculated as

$$I(\nu, \theta) = \delta_{\text{spine}}^3(\theta) I'(\nu/\delta_{\text{spine}}) + \delta_{\text{layer}}^3(\theta) I'(\nu/\delta_{\text{layer}}),$$

where I' is the comoving intensity.

The predicted luminosity trails for the two specific BL Lacs are shown in Fig. 8. Values of Γ_{layer} are set to 1.2 and 1.5 for Mkn 421 and PKS 0735+178 respectively, so that the point of each trail corresponding to the angle $\theta = 60°$ falls approximatively
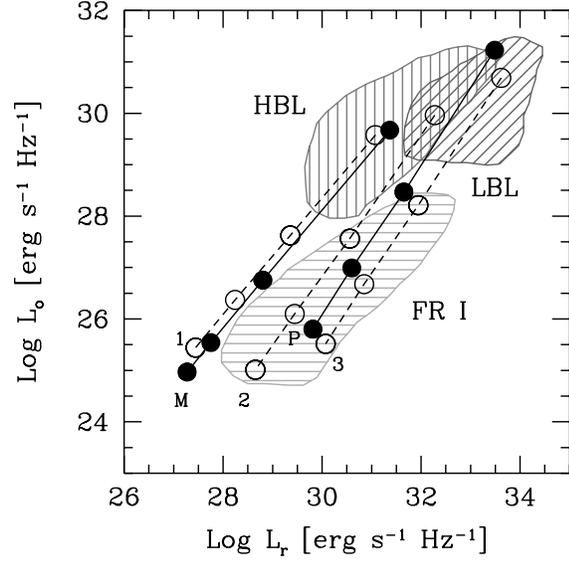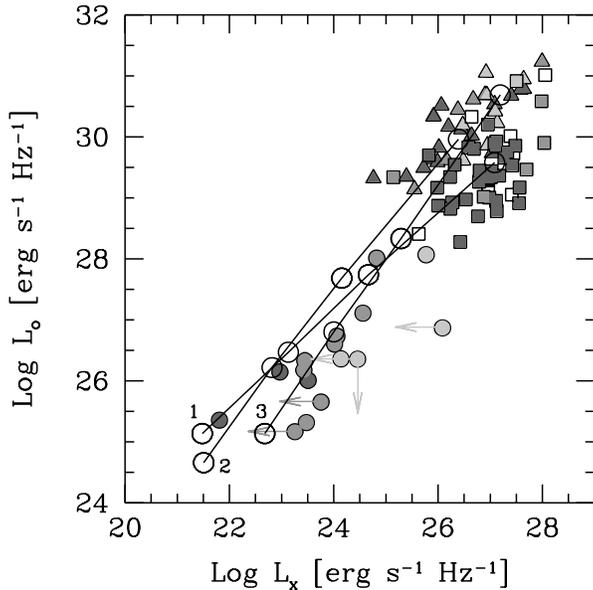

Fig. 8. Debeaming trails in the radio-optical luminosity plane, for the case of the two-velocity jet. The five curves correspond to average SED (1,2 and 3), Mkn 421 (M) and PKS 0735+178 (P). For the average SEDs $\Gamma_{\text{spine}} = 15$ and $\Gamma_{\text{layer}} = 2$; for Mkn 421 $\Gamma_{\text{spine}} = 20$ and $\Gamma_{\text{layer}} = 1.2$; for PKS 0735+178 $\Gamma_{\text{spine}} = 16$ and $\Gamma_{\text{layer}} = 1.5$. Circles correspond to the predicted optical-radio luminosity for different angles of sight (top to bottom: $\theta = 1/\Gamma$, $10°$, $30°$ and $60°$).
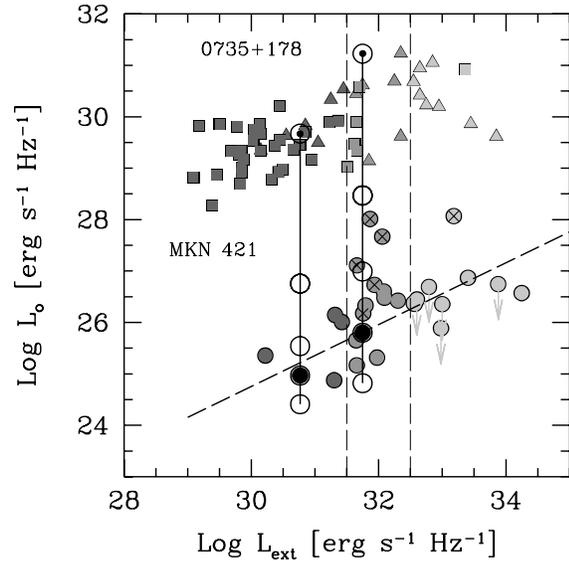
Fig. 9. Debeaming trails for the optical emission of Mkn 421 and PKS 0735+178 in the two-velocity jet scenario. The circles connected by the vertical lines correspond to the sources observed at angles of (top to bottom) $1/\Gamma$, $10°$, $30°$, $60°$ (filled black circles) and $90°$. The values of Γ_{layer} (1.2 for and 1.5 for Mkn 421 and PKS 0735+178, respectively) are chosen in order for the luminosity at $60°$ to correspond to the median value for each bin of extended radio power.

onto the median of the FR I optical core luminosity in each L_{ext} bin (Fig. 9).

By using the same value of Γ_{layer} this two-velocity model satisfactorily predicts the properties of the debeamed counter-

Fig. 10. Debeaming trails in the optical-X-ray luminosity plane for the average BL Lacs SED. Two-velocity jet with $\Gamma_{\mathrm{spine}} = 15$ and $\Gamma_{\mathrm{layer}} = 2$ for all SED. Circles are FR I, squares and triangles represent X-ray and radio selected BL Lacs, respectively. Grey scales correspond to bins of extended radio luminosity, as for Fig. 1. Open triangles and squares are sources without measurement of their extended radio power. Open circles correspond to the predicted optical-X-ray luminosity for different angles of sight (top to bottom: $\theta = 1/\Gamma$, $10°$, $30°$ and $60°$).

parts of LBL and in particular it reproduces the FR I location in the $L_r - L_o$ plane.

Conversely this picture can not account for the observed optical–radio properties of debeamed HBL. The luminosity of objects seen at $\theta = 60°$ is close to the lower limit of the FR I region in the optical, but still one order of magnitude fainter in the radio. We must stress however that the extended radio powers of HBLs correspond more closely to the range covered by the B2 radio galaxies. Clearly, any firm statement on this issue must await for the analysis of the nuclear properties of the B2 sample, but the extrapolation of the 3CR radio-optical correlation does not match the debeamed predicted luminosities of HBL. This result does not depend on the specific value of Γ_{layer} adopted since, as already discussed in Sect. 4, the HBL trails run almost parallel to the radio-galaxies locus.

A further modification of this model is thus required for the HBL unification. Without altering the comoving spectra of the two components, the simplest change is to assume a lower Doppler factor for *spine* in the radio emitting region, as might be the case if the flow slows down between the optical and the radio emitting sites. This would increase the initial slope of the debeaming trail which would rapidly reach the FR I region.

5.1. Constraints from the X–ray observations

The limited angular resolution makes the analysis of X-ray observations of FR I sources less straightforward than in the radio
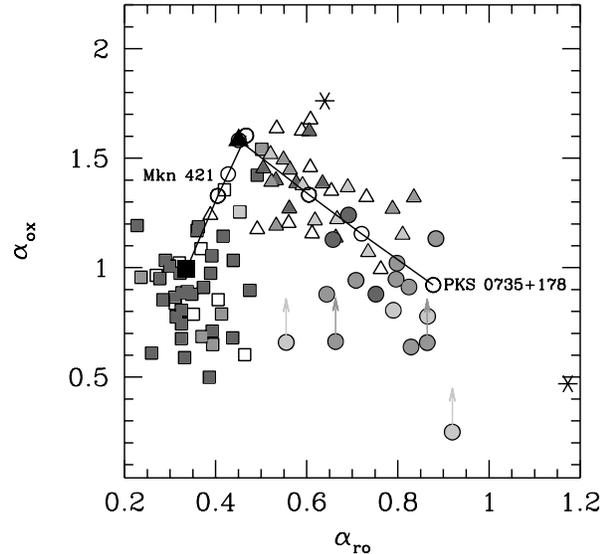
Fig. 11. Debeaming trails in the $\alpha_{\mathrm{ro}} - \alpha_{\mathrm{ox}}$ plane for Mkn 421 and PKS 0735+178. The jet parameters are the same as in Fig. 8. The black filled symbols correspond to the observed BL Lac ($\theta = 1/\Gamma$), while the empty circles represent the predicted position for different angles of sight ($\theta = 10°$, $30°$ and $60°$) in the frame of a two-velocity jet model. The two asterisks indicate sources observed at $\theta = 60°$ in the case of a single emitting component.

and optical bands. In particular it is necessary to disentangle any non thermal nuclear radiation from the often dominant emission of the hot gas associated with the galactic corona and/or galaxy cluster. Nonetheless they provide useful constraints to high energy nuclear emission of these radio-galaxies.

We can test the validity of the two-velocity jet scenario by considering also this X-ray emission. In Fig. 10 we report the debeaming trails in the $L_X - L_o$ plane for the average SEDs assuming the same jet parameters as before: the predicted powers in both bands appear to be consistent with the observed properties of radio galaxies, supporting the presence of a less beamed plasma component (layer) dominating the emission in the parent population also in the X-ray band. Conversely, there is no need for a different amount of beaming in these two bands. This is somehow reassuring, as optical and X–ray are believed to originate co–spatially.

In addition, X–ray data can be used to define the location of radio–galaxies also in the broad band spectral indices plane. The spectral characteristics of blazars are often represented in the plane defined by α_{ro} (5GHz-5500 Å) and α_{ox}(5500 Å-1 keV). It is therefore worthwhile to determine how relativistic beaming affects the position of the objects also in this plane. While an approximated relation between the BL Lacs and FR I broad band spectral slopes is derived in A in the case of constant local spectral indices, changes in the local spectral slopes are properly taken into account.

In this plane (Fig. 11), as already well established, HBL and LBL occupy the left (i.e. flatter α_{ro}) and the top-center (i.e. steeper α_{ox}) regions, respectively and their different position is accounted for by their different SEDs (e.g. Fossati et al.

1998), i.e. reflects the position of the peak of the emission. The FR I region is instead well defined at the center of the diagram. The debeaming trails for Mkn 421 and PKS 0735+178 are also shown[5]: the empty circles correspond to $\theta = 1/\Gamma$, $10° 30°$, $60°$ in the case of the two components model, while the two asterisks represent each source as observed at $60°$ in the case of a single emitting region. PKS 0735+178 falls in the radio galaxy region for $\Gamma_{\text{layer}} = 3$ or less, while Mkn 421 does not intersect this area either in the single or in two component models, confirming the results of the analysis presented above.

6. Summary and conclusions

With the aim of exploring the viability of the unification scenario between (HBL, LBL) BL Lacs and FR I radio galaxies we have compared their nuclear emission in the radio, optical and X–ray bands.

We have firstly considered these spectral regions separately, comparing the nuclear emission of the two classes of objects for similar extended radio power. As the core radiation of BL Lacs is enhanced by relativistic beaming, we derived the bulk Lorentz factors requested to account for the observed distribution. The values of Γ thus inferred are not compatible with the higher bulk velocities requested by theoretical arguments, such as the pair production opacity and the spectral modeling of the SED of BL Lacs.

We then examined the core emission of three samples in the $L_r - L_o$ plane. In the frame of the simplest one-zone emission model, we calculated debeaming trails of the BL Lac broad band emission as predicted by the relativistic transformation for an increasing angle of sight. We found that the model does not account for the observed spectral properties of FR I, as expected from the above inconsistency of the Lorentz factors.

The simplest and rather plausible hypothesis to account for this discrepancy within the unification scenario is to assume a structure in the jet velocity field, in which a fast spine is surrounded by a slow layer. Note however that the slower jet component must be relativistic in order to explain the anisotropic radiation of radio galaxy cores (e.g. Capetti & Celotti 1999). The observed flux is dominated by the emission from either the spine or the slower layer, in the case of aligned and misaligned objects, respectively.

Interestingly, the existence of velocity structures in the jet has been suggested by various authors (Komissarov 1990, Laing 1993) in order to explain some observed properties of FR I (and FR II) jets, such as the structure of the magnetic field in FR I which appears to be longitudinal close to the jet axis and trans-

verse at the edges. Swain et al. 1998 obtained VLA images of 3C 353 (an FR II with straight jets), finding that a model consisting in a fast relativistic spine ($\beta > 0.8$) plus a slower outer layer ($\beta < 0.5$, but still relativistic in order to produce the observed jet-counterjet intensity asymmetry) could account for the apparently lower emissivity near the jet axis. Similar behaviours have been inferred for the two low luminosity radio galaxies M 87 (Owen et al. 1989) and B2 1144+35 (Giovannini et al. 1999). Furthermore, Laing et al. (1999) showed that the jet asymmetries in FR I can be explained by means of a two-speed model. As a consequence, they argued that the lower velocity component dominates in the cores of the edge-on sources, while the fast spine emission dominates the end-on ones. This possibility might be also supported by recent numerical simulations of relativistic jets (Aloy et al. 2000).

The same indication has been found through different approaches. Capetti & Celotti 1999 reveal a trend in the radio galaxy/BL Lac relative powers with the line of sight, which is consistent with a slower (less beamed) component dominating at the largest angles. Capetti et al. 2000 consider the same issue by examining the more detailed SED of five radio galaxies and consider their beamed counterparts. They found that while the spectral shapes of 3C 264 and 3C 270 can be reconducted to those of BL Lacs, the required ratio of beaming factors, i.e. $\delta_{\text{BLLac}}/\delta_{\text{FR I}} \sim 10$–$100$, implies that the corresponding BL Lacs would be overluminous. The inclusion of a slower (less beamed) jet component seems to be a plausible explanation.

We found that Lorentz factors of the layer $\Gamma_{\text{layer}} \sim 2$ can account for the unification of FR I (of the 3CR) with LBL and intermediate luminosity BL Lacs. Instead the debeaming trails for the lowest luminosity HBL do not cross the FR I region in the $L_r - L_o$ plane. While the HBL behavior should be compared with that of radio galaxies with which they share the extended radio power (e.g. those of the B2 catalogue), our simple two-component jet model could not account for the observed properties if the cores of such low-power FR I radio galaxies lied on the extrapolation of the 3CR radio-optical correlation. The properties of such weak sources can be instead reproduced if their radio emitting region is less beamed than the optical one, as could be expected if the jet decelerates after the higher energy emitting zone.

Finally, the presence of velocity structures in jets of course affects the number counts of beamed and unbeamed sources: for example, the lack of BL Lacs in clusters (Owen et al. 1996) could be attributed to values of typical bulk Lorentz factors higher than those derived from statistical arguments (Urry et al. 1991). Intriguingly, the very latter authors had to require a wide distribution of Lorentz factors to account for the number densities of FR I and BL Lacs in the radio band.

Much has still to be understood on the dynamics and emitting properties of relativistic jets. Multifrequency studies of the nuclear properties of beamed sources and their parent populations and their comparison – according to unification scenarios which are well supported by other independent indications – constitute a new and powerful tool to achieve that, both for well studied individual sources as well as complete samples. Near IR

---

[5] Note that again the two trails differ because of the different SEDs: for Mkn 421 the peak of the synchrotron component is between the optical and the X-ray bands and therefore the effect of debeaming is, initially (i.e. for increasing θ) to steepen both α_{ro} and α_{ox}; when the Compton peak enters the X-ray band, α_{ox} flattens. Instead, for PKS 0735+178 the synchrotron peaks between the radio and the optical, and the 1 keV flux is due to Compton and, for the range of angles of sight considered here, the change in the spectral indices turns out to be monotonous.

observations by HST, mm data and higher resolution and sensitivity by Chandra in X–rays will further open this possibility.

Concluding, the radio, optical and X-ray nuclear emission of FR I and BL Lacs strongly indicate the presence of a velocity structure in the jet if indeed these sources are intrinsically identical. In other words, by considering the indications of trends in the SED of blazars emerged in the last few years (Giommi & Padovani 1994, Fossati et al. 1998) together with the constraints derived from their unification with radio galaxies, it appears that the phenomenology of these sources is characterized and determined by differences *both* in the intrinsic SED it and in beaming properties.

Appendix A: debeaming and the broad band spectral slopes

In the case of a one-component model, and under the assumption that the local spectral indices are constant, we can derive the transformation law for the change of the spectral slope due to relativistic beaming. If the flux density in the frame comoving with the emitting region is $F'_{\nu'}$, the observed one is

$$F_\nu^{\mathrm{object}}(\nu) = \delta_{\mathrm{object}}^{p+\alpha} F'_{\nu'}(\nu),$$

where δ_{object} is the beaming factor of the same object for different lines of sight (i.e. observed as BL Lac or as radio galaxy). Substituting these transformations in the definition of the broadband spectral index α_{12} (where 1 and 2 refer to radio, optical or X-ray flux), one obtains

$$\alpha_{12}^{\mathrm{BLLac}} = -\frac{\log\left\{\frac{F_2^{\mathrm{FR\ I}}(\nu_2)(\delta_{\mathrm{BLLac}}/\delta_{\mathrm{FR\ I}})^{p+\alpha_2}}{F_1^{\mathrm{FR\ I}}(\nu_1)(\delta_{\mathrm{BLLac}}/\delta_{\mathrm{FR\ I}})^{p+\alpha_1}}\right\}}{\log(\nu_2/\nu_1)}$$

which can be written as

$$\alpha_{12}^{\mathrm{BLLac}} - \alpha_{12}^{\mathrm{FR\ I}} = (\alpha_1 - \alpha_2)\frac{\log(\delta_{\mathrm{BLLac}}/\delta_{\mathrm{FR\ I}})}{\log(\nu_2/\nu_1)},$$

where α_1 and α_2 are the local spectral indices.

References

Aloy M.-A., Gómez J.-L., Ibáñez J.-M., Martí J.-M., Müller E., 2000, ApJ 528, L85

Antonucci R., 1993, A&AR 31, 473

Antonucci R.R.J., Ulvestad J.S., 1985, ApJ 294, 158

Capetti A., Celotti A., 1999, MNRAS 304, 434

Capetti A., Trussoni E., Celotti A., Feretti L., Chiaberge M., 2000, MNRAS submitted

Celotti A., Maraschi L., Ghisellini G., Caccianiga A., Maccacaro T., 1993, ApJ 416, 118

Celotti A., Fabian A.C., Rees M.J., 1998, MNRAS 293, 239

Chiaberge M., Ghisellini G., 1999, MNRAS 306, 551

Chiaberge M., Capetti A., Celotti A., 1999, A&A 349, 77

Chiaberge M., Capetti A., Celotti A., 2000, A&A 355, 873

Dondi L., Ghisellini G., 1995, MNRAS 273, 583

Elvis M., Plummer D., Schachter J., Fabbiano G., 1992, ApJS 80, 257

Fabbiano G., Trinchieri G., Elvis M., Miller L., Longair M., 1984, ApJ 277, 115

Fanaroff B.L., Riley J.M., 1974, MNRAS 167, 31

Fossati G., Maraschi L., Celotti A., Comastri A., Ghisellini G., 1998, MNRAS 299, 433

Ghisellini G., Maraschi L., 1989, ApJ 340, 181

Ghisellini G., Padovani P., Celotti A., Maraschi L., 1993, ApJ 407, 65

Ghisellini G., Celotti A., Fossati G., Maraschi L., Comastri A., 1998, MNRAS 301, 451

Giommi P., Padovani P., 1994, MNRAS 268, L51

Giovannini G., Feretti L., Gregorini L., Parma P., 1988, A&A 199, 73

Giovannini G., Taylor G.B., Arbizzani E., et al., 1999, ApJ 522, 101

Hardcastle M.J., Worrall D.M., 1999, MNRAS 309, 969

Henkel C., Wang Y.P., Falcke H., Wilson A.S., Braatz J.A., 1998, A&A 335, 463

Kollgaard R.I., Wardle J.F.C., Roberts D.H., Gabuzda D.C., 1992, AJ 104, 1687

Kollgaard R.I., Palma C., Laurent-Muehleisen S.A., Feigelson E.D., 1996, ApJ 465, 115

Komissarov S.S., 1990, SvA Letters 16, 284

Kühr H., Witzel A., Pauliny-Toth I.I.K., Nauber U., 1981, A&AS 45, 367

Laing R.A., 1993, In: Burgarella D., Livio M., O'Dea C.P. (eds.) Space Telescope Sci. Inst. Symp. 6: Astrophysical Jets. Cambridge University Press, Cambridge, p. 95

Laing R.A., Parma P., de Ruiter H.R., Fanti R., 1999, MNRAS 306, 513

Macomb D.J., Akerlof C.W., Aller H.D., et al., 1996, ApJ 459, L111

Maraschi L., Ghisellini G., Celotti A., 1992, ApJ 397, L5

Mastichiadis A., Kirk J.G., 1997, A&A 320,, 19

Murphy D.W., Browne I.W.A., Perley R.A., 1993, MNRAS 264 298

Owen F.N., Ledlow M.J., Keel W.C., 1996, AJ 111, 53

Owen F.N., Hardee P.E., Cornwell T.J., 1989, ApJ 340, 698

Padovani P., 1992, A&A 256, 399

Perlman E.S., Stocke J.T., Schachter J.F., et al., 1996, ApJS 104, 251

Sikora M., Begelman M.C., Rees M.J., 1994, ApJ 421, 153

Sparks W.B., Golombek D., Baum S.A., et al., 1995, ApJ 450, L55

Spinrad H., Djorgovski S., Marr J., Aguilar L., 1985, PASP 97, 932

Stickel M., Fried J.W., Kühr H., Padovani P., Urry C.M., 1991, ApJ 374, 431

Swain M.R., Bridle A.H., Baum S.A., 1998, ApJ 507, L29

Tavecchio F., Maraschi L., Ghisellini G., 1998, ApJ 509, 608

Trussoni E., Vagnetti F., Massaglia S., et al., 1999, A&A 348, 437

Ulrich M.H., 1989, In: Maraschi L., Maccacaro T., Ulrich M.H. (eds.) BL Lac Objects. Springer, Berlin, p. 45

Urry C.M., Falomo R., Scarpa R., et al., 1999, ApJ 512, 88

Urry C.M., Padovani P., 1995, PASP 107, 803

Urry C.M., Padovani P., Stickel M., 1991, ApJ 382, 501

Worral D.M., Birkinshaw M., 1994, ApJ 427, 134